



# RGS9-1 is required for normal inactivation of mouse cone phototransduction

A. L. Lyubarsky,<sup>1</sup> C.-K. Chen,<sup>2</sup> F. Naarendorp,<sup>3</sup> X. Zhang,<sup>4</sup> T. Wensel,<sup>4</sup> M. I. Simon,<sup>5</sup> E. N. Pugh, Jr.<sup>1</sup>

<sup>1</sup>F. M. Kirby Center and Department of Ophthalmology, University of Pennsylvania, Philadelphia, PA; <sup>2</sup>Department of Ophthalmology and Human Genetics, University of Utah, Salt Lake City, UT; <sup>3</sup>Department of Psychology, Northeastern University, Boston, MA; <sup>4</sup>Department of Biochemistry, Baylor College of Medicine, Houston, TX; <sup>5</sup>Division of Biology, California Institute of Technology, Pasadena, CA

**Purpose:** To test the hypothesis that Regulator of G-protein Signaling 9 (RGS9-1) is necessary for the normal inactivation of retinal cones.

**Methods:** Mice having the gene RGS9-1 inactivated in both alleles (RGS9-1 <sup>-/-</sup>) were tested between the ages 8-10 weeks with electroretinographic (ERG) protocols that isolate cone-driven responses. Immunohistochemistry was performed with a primary antibody against RGS9-1 (anti-RGS9-1c), with the secondary conjugated to fluorescein isothiocyanate, and with rhodamine-conjugated peanut agglutinin.

**Results:** (1) Immunohistochemistry showed RGS9-1 to be strongly expressed in the cones of wildtype (WT is C57BL/6) mice, but absent from the cones of RGS9-1 mice. (2) Cone-driven b-wave responses of dark-adapted RGS9-1 <sup>-/-</sup> mice had saturating amplitudes and sensitivities in the midwave and UV regions of the spectrum equal to or slightly greater than those of WT (C57BL/6) mice. (3) Cone-driven b-wave and a-wave responses of RGS9-1 <sup>-/-</sup> mice recovered much more slowly than those of WT after a strong conditioning flash: for a flash estimated to isomerize 1.2% of the M-cone pigment and 0.9% of the UV-cone pigment, recovery of 50% saturating amplitude was approximately 60-fold slower than in WT.

**Conclusions:** (1) The amplitudes and sensitivities of the cone-driven responses indicate that cones and cone-driven neurons in RGS9-1 <sup>-/-</sup> mice have normal generator currents. (2) The greatly retarded recovery of cone-driven responses of RGS9-1 <sup>-/-</sup> mice relative to those of WT mice establishes that RGS9-1 is required for normal inactivation of the cone phototransduction cascades of both UV- and M-cones.

In the phototransduction G-protein-coupled receptor (GPCR) cascades of vertebrate rods and cones, signal amplification is effected primarily by two enzymes: (1) photoactivated visual pigment (R\*), which catalytically generates the activated form of the G-protein (G\* = G<sub>i</sub>α-GTP), and (2) the activated complex (G\*-E\*) of the effector enzyme, phosphodiesterase (E) with G\* [1]. The timely inactivation of these two enzymatic amplifiers after their activation by a light stimulus is necessary for normal visual function, and proteins specialized to inactivate each of them have been found and characterized in rods. Thus, in rods, rhodopsin kinase (GRK1) and arrestin (Arr1) are both necessary for normal inactivation of R\*, and null defects in these latter proteins lead to Oguchi's disease, a form of stationary night blindness in which long-lived decay products of R\* cause rods to recover extremely slowly from light exposure [2,3]. Recently, it has been found that normal inactivation of the G\*-E\* complex in rods requires a GTPase-activating protein or "GAP", RGS9-1, which is expressed only in the retina [4,5]. RGS9-1 has an obligatory requirement for a specific G-protein β-subunit, Gβ5-L, to be stably expressed and present in rod outer segments, where the

complex, RGS9-1/ Gβ5-L, performs its GAP function [6,7]. The rods of mice null for RGS9-1 have extremely slowed photoresponses, recovering from moderate intensity flashes with a dominant time constant (9 s) that is 45-fold longer than that in WT (ca. 0.2 s) [8], and thus these animals have a "stationary night blindness" originating in the slowed inactivation of the second cascade amplifier.

Relatively little is known about the mechanisms of inactivation of cone phototransduction cascades, as compared with what is known about the mechanisms of inactivation in rods. Because the primary proteins of the cascades of cones, the photopigment GPCR, the G-protein, the PDE, and the cyclic nucleotide-gated channel, all are distinct isoforms from those of rods, it might be expected that the inactivating proteins of cones would also be distinct from those in rods. However, recent work has established that the normal inactivation of R\* in murine cones requires GRK1, "rhodopsin kinase", violating this expectation [9], and also that bovine cones strongly express RGS9-1 [10]. Here we test the hypothesis that the GAP factor, RGS9-1 is necessary for normal inactivation of cones in the mouse by examining the cone-driven ERG responses of mice homozygously null for this protein.

## METHODS

**Animals and husbandry:** All experimental procedures were done in compliance with NIH guidelines, as approved by the respective Institutional Animal Care and Use Committees of

Correspondence to: E. N. Pugh, Jr., Ph.D., F. M. Kirby Center for Molecular Ophthalmology, University of Pennsylvania, Stellar-Chance Building, Room 309B, 422 Curie Boulevard, Philadelphia, PA, 19104-6069; Phone: (215) 898-2403; FAX: (215) 898-7155; email: [pugh@mail.med.upenn.edu](mailto:pugh@mail.med.upenn.edu)

the University of Pennsylvania, the California Institute of Technology, and Baylor College of Medicine. RGS9-1  $-/-$  mice were derived at the California Institute of Technology on C57BL/6-129/SvJ background as described elsewhere [8]. C57BL/6 mice were used as controls, and hereafter are referred to as "WT." All animals employed for ERG recordings were born and maintained under controlled ambient illumination on 12/12 light/dark cycle with the illumination level at 2.5 photopic lux as described previously [11,12].

**Immunohistochemistry:** Whole eyes were removed from euthanized WT and RGS9-1  $-/-$  mice and fixed in 4% paraformaldehyde-phosphate buffered saline (PBS, pH 7.2) for 10 to 16 h at 4 °C. After fixing, the eyes were placed in 30% sucrose (w/v)-PBS for 1 h at 4 °C, then embedded in OCT compound Tissue-Tek (Sakura Finetek, Inc., Torrance, CA). Frozen sections were cut 14  $\mu$ m thick, thawed at room temperature for 2 min, post-fixed in 1:1 methanol:acetone (vol/vol) for 10 min, and thereafter processed at room temperature. They were rehydrated in PBS (pH 7.2) for 20 min and blocked with 10% sheep serum (Sigma Chemical, St. Louis, MO) PBS for

1 h. To stain RGS9, tissue sections were incubated with primary antibody to RGS9, anti-RGS9-1c [4], at a 1:200 dilution in 10% sheep serum-PBS. To stain G $\beta$ 5, a polyclonal antibody directed against a peptide epitope [13] common to G $\beta$ 5-L and G $\beta$ 5-S was used, also at a 1:200 dilution in 10% sheep serum-PBS. All sections were incubated with primary antibody overnight in a humidified atmosphere. After being washed 3 x 5 min in PBS, sections were incubated for 1 h with fluorescein isothiocyanate (FITC)-conjugated anti-rabbit immunoglobulin G (Vector, Burlingame, CA), at a 1:25 dilution, and, when included, rhodamine-conjugated peanut agglutinin (Vector) at a 1:100 dilution in 10% sheep serum-PBS in a humidified atmosphere. Peanut agglutinin has been established to bind specifically to cone photoreceptor cells [14]. Sections were washed 3 x 10 min in PBS and mounted in aqueous mounting medium (Gel/Mount; Biomed, Foster City, CA). Sections were examined and photographed with a confocal fluorescence microscope (Zeiss LSM 510) and a Spot digital camera (Diagnostic Instruments, Inc., Sterling Heights, MI), and processed with Adobe Photoshop (v. 5.5).

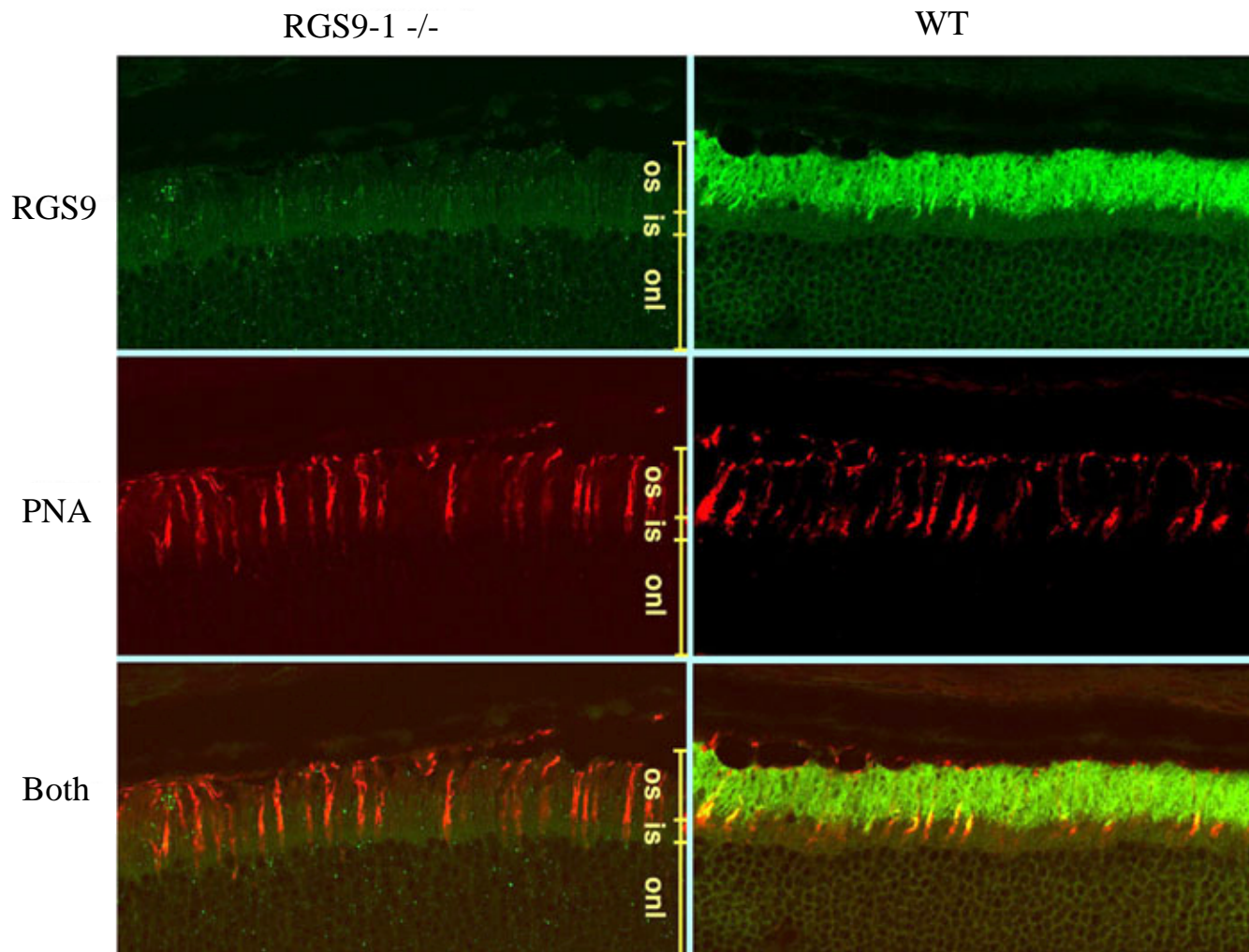


Figure 1. Immunofluorescence staining of RGS9-1 and cones in the mouse retina. Left column: sections from retina of an RGS9-1  $-/-$  mouse. Right column: sections from wildtype (C57BL/6) mouse. "RGS9", staining with fluorescein-isothiocyanate (FITC) conjugated to secondary antibody, with primary against RGS9-1, as described in Methods. "PNA", staining with rhodamine-conjugated peanut agglutinin (red), which binds to cones. The two lowermost panels ("Both") were prepared by digitally summing the fluorescein and rhodamine images.

**Electroretinography:** Electroretinographic (ERG) recordings were made when animals were between 8 and 12 weeks of age. Protocols for ERG recordings, stimulus intensity calibration and computation of the amount of visual pigments isomerized by the flashes, and methods of isolating cone-driven responses are described in detail elsewhere [9,12]. In brief, ERGs were recorded from anesthetized mice with a differential amplifier with bandwidth 0.1 Hz to 1 KHz, and sampled and digitized at 5 KHz. The corneal electrode was a platinum wire, while the reference electrode was a tungsten needle inserted subcutaneously in the forehead. The recording chamber served dually as a Faraday cage and a Ganzfeld, with ports and baffles for illumination. Cone-signal isolation was effected with steady backgrounds estimated to produce 6000 photoisomerizations  $\text{rod}^{-1}\text{s}^{-1}$  in WT mice, and 3000 photoisomerizations  $\text{rod}^{-1}\text{s}^{-1}$  in RGS9-1  $^{-/-}$  mice.

## RESULTS

**Cones of WT mice strongly express RGS9-1:** Figure 1 presents images of WT and RGS9-1  $^{-/-}$  retinas stained to reveal

the expression of RGS9-1. As reported previously, RGS9-1 antibody ("RGS9") binds strongly in the outer segment layer [4] in WT, but not in RGS9-1  $^{-/-}$  retinas. Peanut-agglutinin ("PNA") staining reveals cones at approximately the same density in normal and RGS9-1 null retinas: counts of 3 sections of 2 mice of each type yielded  $2.5 \pm 0.5$  (mean  $\pm$  s.d.) cones per  $20 \mu\text{m}$  (RGS9-1  $^{-/-}$ ) and  $2.7 \pm 0.2$  cones per  $20 \mu\text{m}$  (WT). Given that the sections are  $15 \mu\text{m}$  thick, the cone density is estimated to be about 3 cones per  $(20 \mu\text{m} \times 15 \mu\text{m}) = 300 \mu\text{m}^2$ , or 1 cone per  $100 \mu\text{m}^2$ . Since the density of rods in rodent retinas is about 1 per  $3 \mu\text{m}^2$ , cones constitute about 3% of the photoreceptors in these retinas. The superposition of the images generated with the antibody and the peanut agglutinin ("PNA") confirms the strong expression of RGS9-1 in the cones of WT mice, as found previously in bovine cones [10], and absence of RGS9-1 in the knockout mice. No RGS9-1 expression could be reliably detected outside the photoreceptor layer.

Figure 2 compares WT and RGS9-1  $^{-/-}$  retinas for the expression of G $\beta$ 5, and shows that G $\beta$ 5 is very greatly re-

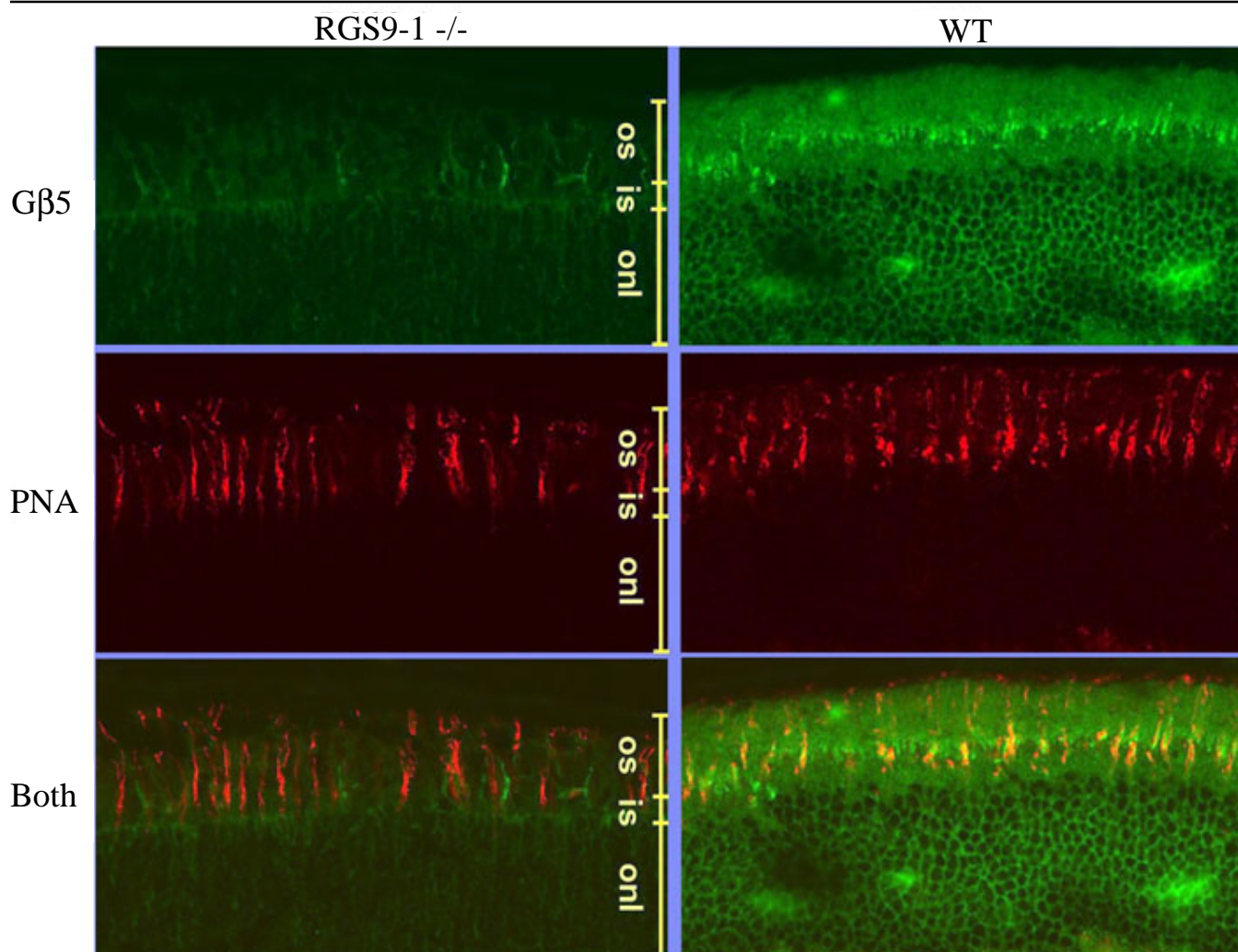


Figure 2. Immunofluorescence staining of G $\beta$ 5 and cones in the mouse retina. Left column: section from retina of an RGS9-1  $^{-/-}$  mouse. Right column: sections from wildtype (C57BL/6) mouse. "G $\beta$ 5", staining with fluorescein-isothiocyanate (FITC) conjugated to secondary antibody, with primary against G $\beta$ 5, as described in Methods. "PNA", staining with rhodamine-conjugated peanut agglutinin (red), which binds to cones. The two lowermost panels ("Both") were prepared by digitally summing the fluorescein and rhodamine images.

duced or absent in the outer layers of the retina of RGS9-1  $-/-$  mice, and in particular, missing from the PNA-stained cones.

*Rods of dark-adapted RGS9-1  $-/-$  mice generate nearly normal circulating currents in situ but are very slow to recover from strong light stimuli:* Figure 3 shows ERGs elicited from a WT and a RGS9-1  $-/-$  mouse with a flash estimated to isomerize  $\sim 1\%$  of the rhodopsin. The traces of Figure 3A,C, were obtained when the animals were dark-adapted overnight, for at least 12 h. The initial corneal-negative component of these traces is the a-wave (violet-highlighted portion of traces). The immediately following positive-going potential is a mixture of the rod- and cone-driven b-waves, and oscillatory potentials. Measured as in Figure 3A,C, the saturating a-wave amplitude of dark-adapted RGS9-1  $-/-$  mice ( $248 \pm 66 \mu\text{V}$ ,  $n=19$ ) was indistinguishable from that of WT C57BL/6 mice ( $243 \pm 70 \mu\text{V}$ ,  $n=16$ ). In WT mice, more than 95% of the saturating a-wave amplitude results from suppression of rod circulating current [11,12]. Thus, the rods of fully dark-adapted RGS9-1  $-/-$  mice generate circulating currents of normal magnitude, consistent with previous evidence from suction electrode recordings of isolated rods [8].

In contrast to its normal amplitude, the recovery of the a-wave of RGS9-1  $-/-$  mice was greatly retarded relative to that in WT. In the experiments of Figure 3, after exposure to the initial flash, the mice were left to dark adapt for 2 min and then stimulated again with the same flash (traces of Figure 3C,D). Whereas the ERG of the WT mouse had a completely recovered a-wave (and thus, rod circulating current), that of the RGS9-1  $-/-$  mouse exhibited only a very small a-wave ( $\sim 10 \mu\text{V}$ ; red highlight), and a corneal-positive b-wave of substantially reduced-amplitude. Previous analysis has shown that the ERGs recorded under conditions such as illustrated in Figure 3D originate exclusively from cone-driven neurons; we now proceed to characterize such responses in RGS9-1  $-/-$  mice.

*Both UV and M-cone-driven retinal responses are functional in RGS9-1  $-/-$  mice:* WT mice have both midwave (M)-

sensitive ( $\lambda_{\text{max}} \approx 510 \text{ nm}$ ) and UV-sensitive cones ( $\lambda_{\text{max}} \approx 355 \text{ nm}$ ) [12,15,16], so we inquired as to whether the sensitivity of the cone-driven b-wave responses of RGS9-1  $-/-$  animals are comparable to those of WT mice. Figure 4 presents two series of ERGs from an RGS9-1  $-/-$  mouse, elicited by monochromatic 361 and 513 nm flashes of varied intensity under cone-isolation conditions. The amplitudes of the b-wave responses

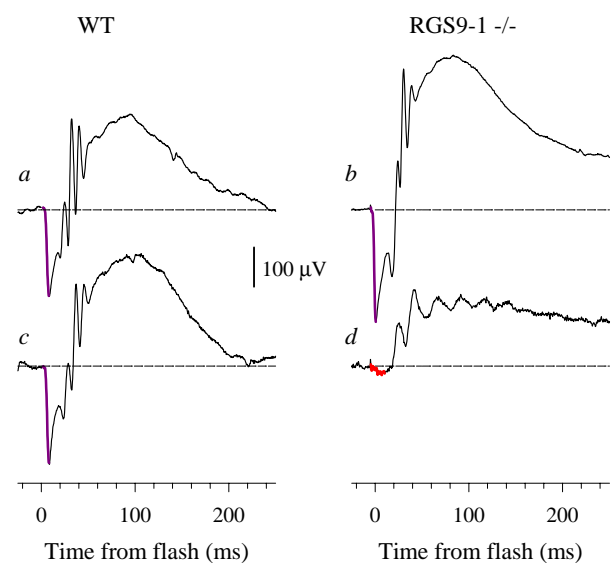


Figure 3. ERGs from WT and RGS9-1  $-/-$  mice. A white flash isomerizing  $\sim 1\%$  of the rhodopsin in the retina was delivered in a Ganzfeld to each dark-adapted animal, generating responses seen in panels A and B. The response to the same flash was then recorded again after 2 min in darkness (panels C and D). The initial corneal-negative component highlighted in violet in panels A-C and in red in panel D is the a-wave, while the corneal-positive deflections that follow (and truncate) the a-wave are a mixture of rod- and cone-driven b-waves and the so-called oscillatory potentials [29].

TABLE 1. PARAMETERS OF CONE-DRIVEN ELECTRORETINOGRAMS OF WT AND RGS9-1  $-/-$  MICE

Parameter	$a_{\text{max}}$	$b_{\text{max}}$	$S_{\text{M}}$	$S_{\text{UV}}$	$S_{\text{UV}} / S_{\text{M}}$
Unit	$\mu\text{V}$	$\mu\text{V}$	$(\text{photons } \mu\text{m}^{-2})^{-1} \times 10^5$	$(\text{photons } \mu\text{m}^{-2})^{-1} \times 10^5$	
WT (C57BL/6)*	$21 \pm 10$	$100 \pm 36$	$3.0 \pm 2.0$	$17 \pm 12$	$5.2 \pm 1.8$
$n$	9	11	7	6	6
RGS9-1 $-/-$	$16 \pm 5$	$156 \pm 38$	$6.7 \pm 0.8$	$19 \pm 3$	$3.0 \pm 0.9$
$n$	7	7	7	7	7

The top row identifies a measured or computed parameter of cone-driven ERGs.  $a_{\text{max}}$  is the saturating amplitude of the a-wave component (cf. Figure 3D and Figure 4, red traces, and Figure 7).  $b_{\text{max}}$  is the saturating amplitude of the Gaussian-filtered b-wave, obtained under cone-isolation conditions (Figure 4A).  $S_{\text{M}}$  and  $S_{\text{UV}}$  are the relative sensitivities of the cone-driven b-wave in the midwave and UV spectral regions, as illustrated in Figure 5. These sensitivities specify the fraction of the saturated response generated per  $(\text{photon } \text{mm}^{-2})$  at the cornea. Thus, for the WT mouse, a 360 nm (UV) flash generates a peak fractional response of  $3 \times 10^{-5}$  or 0.003% per  $(\text{photon } \text{mm}^{-2})$  at the cornea. The ratio  $S_{\text{UV}} / S_{\text{M}}$  was determined separately for each animal. The errors given are standard deviations. \*Data of C57BL/6 mice are taken from Table 1 of reference [9].

were extracted from filtered traces (smooth colored or gray curves). This was done to obviate potential artifacts that the oscillatory potentials might cause in estimation of b-wave amplitudes (compare WT and RGS9-1  $-/-$  traces in Figure 3). The saturating amplitudes of the cone-driven b-waves for RGS9-1  $-/-$  mice were on average about 50% larger than for WT animals, though this difference is not statistically significant ( $t=1.435$ ,  $p<0.1$ ,  $df=16$ ). The amplitudes of the cone a-waves, which will be described in more detail below (cf. red highlighted early portions of traces in Figure 3), also were not reliably different between RGS9-1  $-/-$  and WT (Table 1).

Intensity-response relations derived from the data of Figure 4, together with data of 6 additional RGS9-1  $-/-$  mice, are shown in Figure 5A. From such data the ratio of the peak spectral sensitivities,  $S_{UV}/S_M$ , of the b-waves driven by the two cone types can be derived [12]. As illustrated in Figure 5B, the sensitivity ratio of the RGS9-1  $-/-$  mice,  $S_{UV}/S_M=3.0$ , is lower than that of WT mice,  $S_{UV}/S_M=5.2$ , but the difference between the ratios is not statistically significant ( $p>0.2$ ,  $df=11$ ). The apparent reason for the decreased sensitivity ratio of the RGS9-1  $-/-$  mice is that their midwave cone sensitivity,  $S_M$ , is higher than that of WT mice (Table 1), suggesting that M-cones or their secondary neurons may be primarily responsible.

*Cone-driven responses of RGS9-1  $-/-$  animals have profoundly slowed recovery from strong flashes:* The paradigm used to investigate the recovery of cone-driven responses is

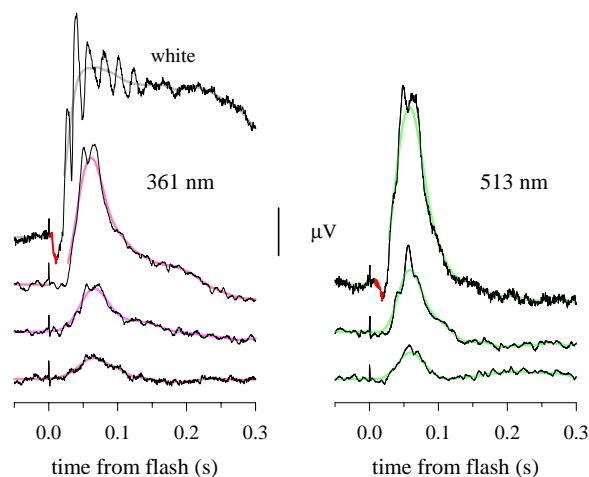


Figure 4. Cone-driven ERGs of an RGS9-1  $-/-$  mouse to 361 and 513 nm flashes of stepped intensity. Each trace is the average of from 3 to 5 individual responses. The intensities of the 361 nm flashes were (from lowest to highest intensity) 620, 1050, and 6020 photons  $\mu\text{m}^{-2}$  at the cornea. The 513 nm intensities were 2500, 5000, and 25600 photons  $\mu\text{m}^{-2}$  at the cornea. The topmost trace in the “361 nm” column is the response to a white flash estimated to 1.2% of the M-cone pigment and 0.09% of the UV-pigment. The smooth gray traces were obtained by convolving the measured traces with a Gaussian function having a standard deviation of 10 ms (bandwidth at 3 dB, 13.25 Hz); the peak amplitudes extracted from the filtered traces are (in  $\mu\text{V}$ ) 22, 45, 134 (361 nm), 28, 65, 187 (513 nm) and 180 (white). The a-wave component of the responses to the two strongest flashes has been highlighted in red.

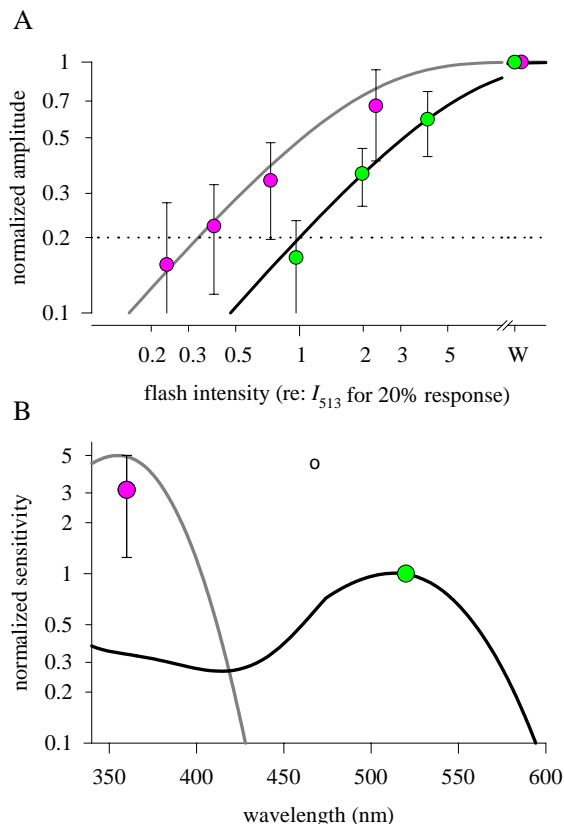


Figure 5. Sensitivity of RGS9-1 mice at the wavelength maxima of the UV- and M-cone pigments. **A:** Averaged amplitude vs. intensity data for RGS9-1  $-/-$  mice ( $n=7$ ) obtained with flashes of 361 nm (pink symbols) and 513 nm (green symbols), under cone-isolation conditions, as in Figure 4; the error bars are 90% confidence intervals. Peak amplitudes were measured after filtering the responses at 13 Hz to remove oscillations (see Methods). The peak amplitudes were normalized by dividing them by the saturating amplitude, obtained in response to the “white” flash (“W” on abscissa). The flash intensities were scaled by a single, common factor: this factor is the intensity at 513 nm ( $I_{513}$ ) estimated by linear interpolation to produce a response of 20% saturated amplitude (dotted line). Saturation functions (thickened black and gray curves), having the form  $r_{\text{peak}}/r_{\text{max}} = 1 - \exp(-kS_{\lambda}I_{\lambda})$  have been plotted through the data, where  $I_{\lambda}$  is the scaled flash intensity,  $S_{\lambda}$  is a wavelength-dependent sensitivity factor and  $k=0.22$ . The black curve was arranged to intercept the dotted line at the abscissa value 1.0, and thus has been positioned so that  $S_{513}=1$ . The gray curve is shifted left by the average relative sensitivity of cone-driven responses of the RGS9-1  $-/-$  mice to these two wavelengths, i.e., by the logarithm of the sensitivity ratio  $S_{UV}/S_M = S_{361}/S_{513}=3.0$  (Table 1). **B:** The spectral sensitivity of cone-isolated b-wave responses of RGS9-1  $-/-$  compared to WT. For each RGS9-1  $-/-$  mouse, the lateral shift (in logarithmic units) between the two saturation functions best fitting its 513 nm and 361 nm data was measured. The point plotted at  $\sim 361$  nm is the mean  $\pm 95\%$  confidence interval of these shifts; the point at 513 nm identifies the normalization position. The solid line gives the spectral sensitivities of the UV- and M-cone-driven b-wave responses of WT mice normalized to the sensitivity at 508 nm, as derived in [12].

illustrated in Figure 6. A conditioning flash sufficiently intense to temporarily suppress all cone-driven activity was followed at different interstimulus intervals (ISIs) by a probe flash of the same intensity. Recovery of the cone-driven responses of the WT mouse was found to be complete in about 1 s; in contrast, in the RGS9-1  $-/-$  mouse, the first sign of recovery appeared only after 5 s, and complete recovery required about 100 s.

*The cone-driven a-wave also recovers very slowly:* Because the corneal-positive component of the ERG (the b-wave) represents field potentials generated mostly by second order neurons (reviewed in [11]), and because RGS9-1 is expressed in cones, a question of special interest is whether the slowed recovery was caused by prolonged activation of the cones themselves, or only due to prolonged activity in neurons downstream from the photoreceptors. To address this question we examined the behavior of the cone a-wave, which is thought to originate primarily in the suppression of cone photoreceptor circulating current [17-19], and which we have previously

characterized in C57BL/6 mice [9,12]. Thus, in Figure 7 the initial portions of records from mice stimulated as in Figure 6 have been replotted on expanded time and amplitude scales to facilitate examination of the cone a-wave. Here the differences between the WT and mutant animals in the recoveries of the cone a-waves are seen to parallel the recoveries of the cone-driven b-wave in Figure 6. Caution is called for in identifying cone photoreceptors as the sole underlying generators of the cone-driven a-wave since the primate photopic a-wave has been shown to have a component originating in off-bipolar cells [20,21] and mice have been confirmed to have at least two types of cone off-bipolar cells (Dr. Peter Sterling, University of Pennsylvania, personal communication). However, since cone off-bipolars are driven through an ionotropic glutamate synaptic contact with cones, one can expect their light-stimulated currents to closely track the cone responses.

Figure 8 summarizes the results of applying the protocol of Figure 6 and Figure 7 to populations of WT and RGS9-1  $-/-$  mice. Figure 8A plots the saturated amplitude of the cone-driven b-wave, as a function of time after the conditioning

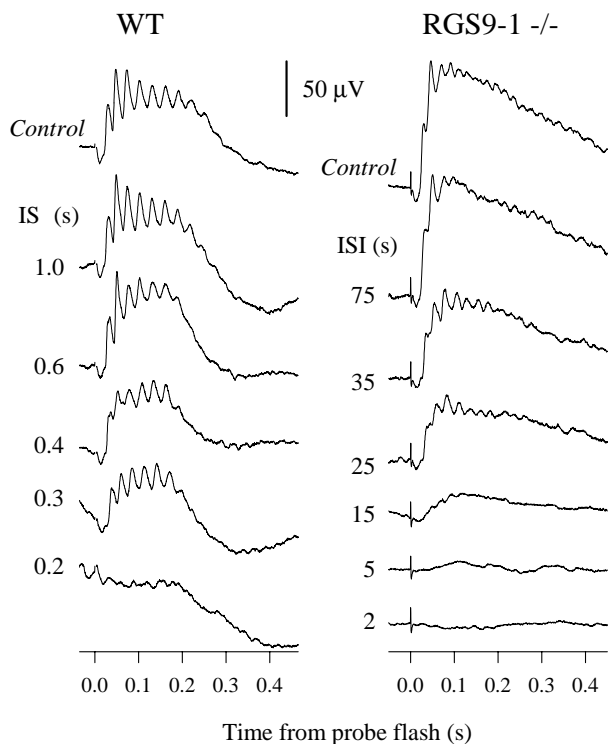


Figure 6. Recovery of cone-driven ERGs after a strong conditioning flash in WT and RGS9-1  $-/-$  mice. Responses to white “probe” flashes isomerizing  $\sim 1.2\%$  of the M-cone pigment and  $\sim 0.9\%$  of the UV-pigment delivered at various interstimulus intervals (ISIs) after an initial flash of the same intensity. Responses obtained without immediately preceding conditioning flashes are identified as “Control”. The control records were obtained with an orange ( $\lambda > 530$  nm) steady background that produced  $\sim 6000$  photoisomerizations rod $^{-1}$ s $^{-1}$  for the WT animal and  $\sim 3000$  for the RGS9-1  $-/-$  mouse to completely suppress rod signals [12]; for all other recordings rod activity was suppressed with the conditioning flash. Each trace is the average of 5-10 records. A time gap of 3.5 ms containing a flash artifact has been omitted from the traces of the WT mouse.

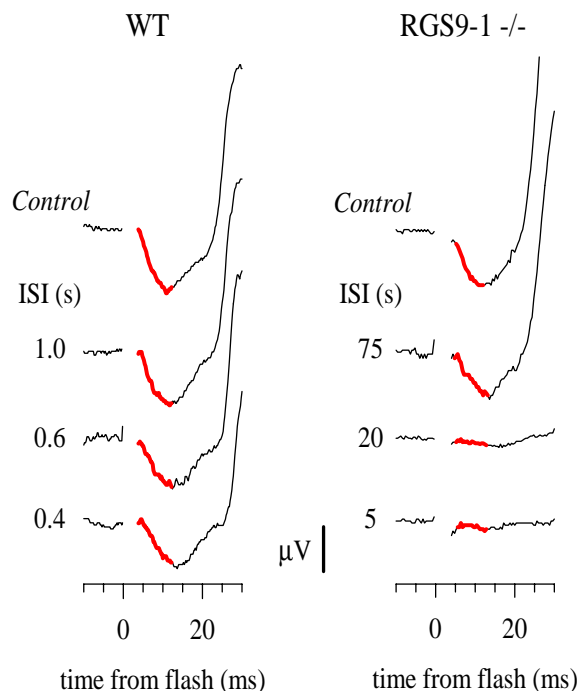


Figure 7. Recovery of the a-wave component of the ERG under cone isolation conditions for WT and RGS9-1  $-/-$  mice. The experimental design and format of presentation were as for the results presented in Figure 6, except that the time base and amplitude scales have been expanded to reveal the initial, corneal-negative portion of the responses. In each panel, the portion of the traces identified with the suppression of cone circulating current, i.e., the cone a-wave, has been emphasized by thickening of the trace and coloring it red. The traces of the WT mouse are the same as those shown in Figure 6; those of the RGS9-1  $-/-$  mouse were taken from a different animal from that of Figure 6, obtained in an experiment arranged to minimize the flash artifact. Each trace is the average of 10-15 records. (For clarity, a time gap of 3.5 ms containing the flash artifact has been omitted from the traces.)

flash. Taking 0.4 s as the average time for the b-wave of WT mice to recover 50% of their dark-adapted amplitude, the cone b-wave of the RGS9-1  $-/-$  mice is seen to recover almost 60-fold more slowly. Figure 8B plots the recovery of the cone a-wave, on a common abscissa with panel A. Again, using the recovery to 50% amplitude as a benchmark, the cone a-waves of the RGS9-1  $-/-$  mice are seen to recover about 60-fold more slowly than those of WT mice.

## DISCUSSION

Observations made with the rod a-wave in this investigation (Figure 3A) are consistent with the hypothesis that RGS9-1 and G $\beta$ 5-L are essential for normal inactivation of rod

transducin, confirming previous findings showing that single rods of RGS9-1  $-/-$  mice exhibit profoundly slowed recovery of their photoresponses [8].

Our results support the conclusion that RGS9-1  $-/-$  mice have a major defect in the inactivation of their cone phototransduction cascades, as follows. First, we have found RGS9-1 to be expressed in murine cones (Figure 1), as previously reported for bovine cones [10]. Second, the greatly slowed recoveries of the a-wave component of the ERG of RGS9-1  $-/-$  mice recorded under cone-signal isolation conditions (Figure 7, Figure 8B) point to a cone-cell locus for the recovery deficit.

Our results show that RGS9-1  $-/-$  mice, like WT mice, have both UV- and M-cones, and secondary neurons driven by these cones (Figure 3, Figure 4), and support the conclusion that RGS9-1 is a GAP factor for cone transducin in both types of cones. This follows since all cone-driven activity of RGS9-1  $-/-$  mice is greatly retarded in recovery from strong flashes (Figure 6, Figure 7). It is noteworthy in this context that only a single cone-specific transducin  $\alpha$ -subunit, GNAT2, has been identified in the GenBank database, including human (Z18859) and murine (NM\_008141) homologs.

It is interesting to compare the effects of inactivating the primary shutoff mechanisms of phototransduction in cones, viz., the GRK1-dependent inactivation of cone R\* and the RGS9-1-G $\beta$ 5-dependent inactivation of the G\*-E\* complex. Cone a-wave and b-wave responses of GRK1  $-/-$  mice, when tested under the same conditions used in this investigation, reach 50% recovery in about 19 s [9], which is comparable to the recovery half-time of 23 s in RGS9-1  $-/-$  mice (Figure 7). Thus, though these inactivating proteins work at distinct stages of the cone transduction cascades, their deletions produce defects in recovery of comparable magnitude.

While the primary proteins of the transduction cascades of cones are established to be distinct isoforms from those of rods. Many of the proteins involved in activation and recovery are shared. The list of shared proteins established to function in both cell types now includes GRK1 (mice; [9], RGS9-1 (this paper)) and guanylyl cyclase, GC1 (GC-E) [22,23]. In addition, the guanylyl cyclase activating protein, GCAP1, has been established to be present in both rods and cones of mice [24]. Given the established capacity of GCAP1 to activate GC1 (reviewed in [25-27]), and its likely role in autosomal dominant cone dystrophy [28], it seems certain that GCAP1 also functions in both cell types. Our results add RGS9-1 to this

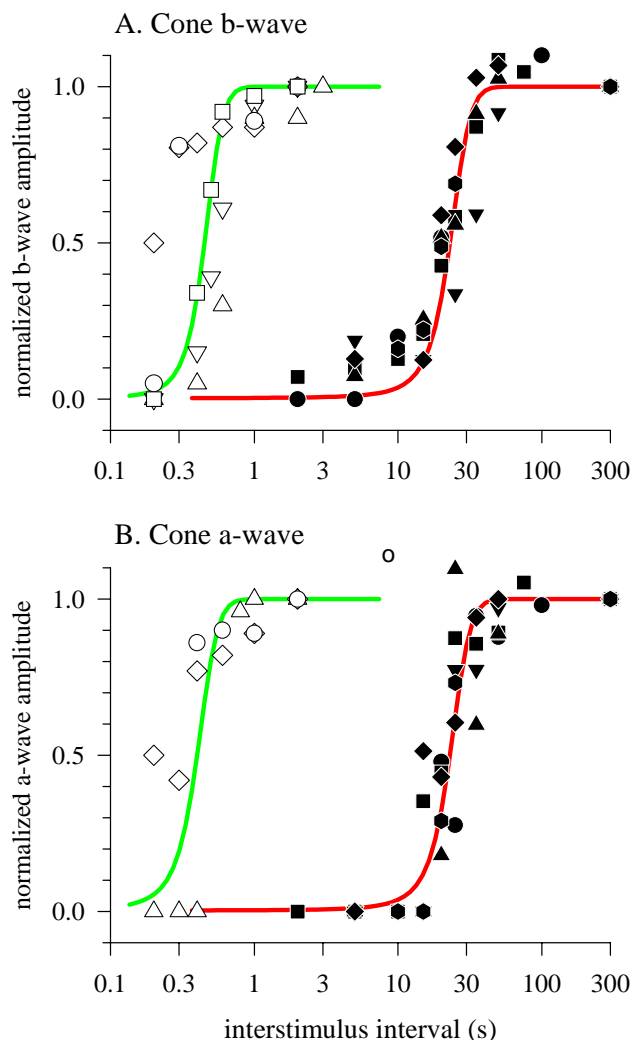


Figure 8. Time course of recovery of cone b-wave and cone a-wave from a strong conditioning flash. **A:** Normalized amplitudes of cone-driven b-waves for WT (open symbols,  $n=5$ ), and RGS9-1  $-/-$  mice (filled symbols,  $n=6$ ) plotted as function of the interstimulus interval (ISI) between the conditioning and probe flashes. **B:** Normalized amplitudes of cone a-waves plotted as a function of the ISI for 3 WT and 5 RGS9-1  $-/-$  mice. The same symbols are used in panels A and B for the data of the same animal. The normalization in each panel was based on the amplitude of the responses at an ISI of 2 or 3 s for WT, and at an ISI of 300 s for RGS9-1  $-/-$  mice. All data in the two panels were collected with the experimental protocols illustrated in Figure 6 and Figure 7. The colored curves have the formula  $\text{amplitude}(t)=1/(1+\exp(-(t-t_{1/2})/\tau))$ , so that  $t_{1/2}$  is the time of 50% recovery, and  $t_{1/2} \pm 2.3\tau$  is approximately the time from 10% to 90% recovery. This same function has been used to describe the recovery of human ERG a-waves [30]. In panel A, the parameter values for WT (green curve) are  $t_{1/2}=0.45$  s and  $\tau=0.07$  s. The parameter values for RGS9-1  $-/-$  (red curve) are  $t_{1/2}=4.0$  s and  $\tau=23$  s. The parameter values used for the curves in panel B are the same, except  $t_{1/2}=0.40$  s for WT. (Accurate estimation of the a-wave recovery in WT mice is difficult at times earlier than 0.3 s, because oscillatory potentials triggered by the initial, conditioning flash can have comparable magnitude to the cone a-wave; see Figure 6 “Control” response.)

growing list of regulatory proteins of phototransduction shared by rods and cones.

### ACKNOWLEDGEMENTS

Supported by NIH grants to ENP, TGW, and MIS, and by awards from the Research to Prevent Blindness Foundation to ENP and TGW. We thank Ann Milam (Department of Ophthalmology, University of Pennsylvania) and Trevor Lamb (Department of Physiology, University of Cambridge), and the reviewers, for helpful comments.

### REFERENCES

- Pugh EN Jr, Lamb TD. Phototransduction in vertebrate rods and cones: molecular mechanisms of amplification, recovery and light adaptation. In: Stavenga DG, de Grip WJ, Pugh EN Jr, editors. *Molecular mechanisms in visual transduction*. Amsterdam: Elsevier; 2000. p. 183-255.
- Yamamoto S, Sippel KC, Berson EL, Dryja TP. Defects in the rhodopsin kinase gene in the Oguchi form of stationary night blindness. *Nat Genet* 1997; 15:175-8.
- Cideciyan AV, Zhao X, Nielsen L, Khani SC, Jacobson SG, Palczewski K. Null mutation in the rhodopsin kinase gene slows recovery kinetics of rod and cone phototransduction in man. *Proc Natl Acad Sci U S A* 1998; 95:328-33.
- He W, Cowan CW, Wensel TG. RGS9, a GTPase accelerator for phototransduction. *Neuron* 1998; 20:95-102.
- Cowan CW, Wensel TG, Arshavsky VY. Enzymology of GTPase acceleration in phototransduction. *Methods Enzymol* 2000; 315:524-38.
- Makino ER, Handy JW, Li T, Arshavsky VY. The GTPase activating factor for transducin in rod photoreceptors is the complex between RGS9 and type 5 G protein beta subunit. *Proc Natl Acad Sci U S A* 1999; 96:1947-52.
- Kovoor A, Chen CK, He W, Wensel TG, Simon MI, Lester HA. Co-expression of Gbeta5 enhances the function of two Ggamma subunit-like domain-containing regulators of G protein signaling proteins. *J Biol Chem* 2000; 275:3397-402.
- Chen CK, Burns ME, He W, Wensel TG, Baylor DA, Simon MI. Slowed recovery of rod photoresponse in mice lacking the GTPase accelerating protein RGS9-1. *Nature* 2000; 403:557-60.
- Lyubarsky AL, Chen C, Simon MI, Pugh EN. Mice lacking G-protein receptor kinase 1 have profoundly slowed recovery of cone-driven retinal responses. *J Neurosci* 2000; 20:2209-17.
- Cowan CW, Fariss RN, Sokal I, Palczewski K, Wensel TG. High expression levels in cones of RGS9, the predominant GTPase accelerating protein of rods. *Proc Natl Acad Sci U S A* 1998; 95:5351-6.
- Pugh EN Jr, Falsini B, Lyubarsky AL. The origin of the major rod- and cone-driven components of the rodent electroretinogram and the effect of age and light-rearing history on the magnitude of these components. In: Williams TP, Thistle AB, editors. *Photostasis and related phenomena*. New York: Plenum Press; 1998. p. 93-128.
- Lyubarsky AL, Falsini B, Pennesi ME, Valentini P, Pugh EN. UV- and midwave-sensitive cone-driven retinal responses of the mouse: a possible phenotype for coexpression of cone photopigments. *J Neurosci* 1999; 19:442-55.
- Watson AJ, Aragay AM, Slepak VZ, Simon MI. A novel form of the G protein beta subunit Gbeta5 is specifically expressed in the vertebrate retina. *J Biol Chem* 1996; 271:28154-60.
- Blanks JC, Johnson LV. Specific binding of peanut lectin to a class of retinal photoreceptor cells. A species comparison. *Invest Ophthalmol Vis Sci* 1984; 25:546-57.
- Calderone JB, Jacobs GH. Regional variations in the relative sensitivity to UV light in the mouse retina. *Vis Neurosci* 1995; 12:463-8.
- Jacobs GH, Neitz J, Deegan JF 2nd. Retinal receptors in rodents maximally sensitive to ultraviolet light. *Nature* 1991; 353:655-6.
- Hood DC, Birch DG. Phototransduction in human cones measured using the alpha-wave of the ERG. *Vision Res* 1995; 35:2801-10.
- Cideciyan AV, Jacobson SG. An alternative phototransduction model for human rod and cone ERG a-waves: normal parameters and variation with age. *Vision Res* 1996; 36:2609-21.
- Smith NP, Lamb TD. The a-wave of the human electroretinogram recorded with a minimally invasive technique. *Vision Res* 1997; 37:2943-52.
- Sieving PA, Murayama K, Naarendorp F. Push-pull model of the primate photopic electroretinogram: a role for hyperpolarizing neurons in shaping the b-wave. *Vis Neurosci* 1994; 11:519-32.
- Bush RA, Sieving PA. Inner retinal contributions to the primate photopic fast flicker electroretinogram. *J Opt Soc Am A* 1996; 13:557-65.
- Robinson SW, Garbers DL. Genetic models to study guanylyl cyclase function. *Methods Enzymol* 2000; 316:558-64.
- Yang RB, Robinson SW, Xiong WH, Yau KW, Birch DG, Garbers DL. Disruption of a retinal guanylyl cyclase gene leads to cone-specific dystrophy and paradoxical rod behavior. *J Neurosci* 1999; 19:5889-97.
- Howes K, Bronson JD, Dang YL, Li N, Zhang K, Ruiz C, Helekar B, Lee M, Subbaraya I, Kolb H, Chen J, Baehr W. Gene array and expression of mouse retina guanylate cyclase activating proteins 1 and 2. *Invest Ophthalmol Vis Sci* 1998; 39:867-75.
- Polans A, Baehr W, Palczewski K. Turned on by Ca<sup>2+</sup>! The physiology and pathology of Ca(2+)-binding proteins in the retina. *Trends Neurosci* 1996; 19:547-54.
- Pugh EN, Duda T, Sitaramayya A, Sharma RK. Photoreceptor guanylate cyclases: a review. *Biosci Rep* 1997; 17:429-73.
- Dizhoor AM, Hurley JB. Regulation of photoreceptor membrane guanylyl cyclases by guanylyl cyclase activator proteins. *Methods* 1999; 19:521-31.
- Dizhoor AM, Boikov SG, Olshevskaya EV. Constitutive activation of photoreceptor guanylate cyclase by Y99C mutant of GCAP-1. Possible role in causing human autosomal dominant cone degeneration. *J Biol Chem* 1998; 273:17311-4.
- Wachtmeister L. Oscillatory potentials in the retina: what do they reveal? *Prog Retin Eye Res* 1998; 17:485-521.
- Thomas MM, Lamb TD. Light adaptation and dark adaptation of human rod photoreceptors measured from the a-wave of the electroretinogram. *J Physiol* 1999; 518:479-96.

The print version of this article was created on 20 Mar 2001. This reflects all typographical corrections and errata to the article through that date. Details of any changes may be found in the online version of the article.